

ADVANCED MARTENSITIC STAINLESS STEELS FOR DENTAL INSTRUMENTS

P. D. Dolzhenko,¹ R. V. Mishnev,¹ R. O. Kaibyshev,² and A. N. Belyakov¹

UDC 669.018.2

The developed microstructures and tensile strength of AISI 420-type martensitic stainless steels with different carbon content from 0.2 to 0.4% were studied after tempering at 450°C for 3 h and at 800°C for 16 h. The volume fraction of retained austenite depends significantly on the carbon content. The fraction of retained austenite is about 0.3 after tempering at 450°C for 3 h in steels with 0.3–0.4% carbon. An average grain size comprises 0.97 μm and 0.6 μm after tempering at 450°C for 3 h in the steels with carbon content of 0.2 and 0.4%, respectively. Tempering at 800°C for 16 h increases the grain size to 2.1 μm in the 0.2% C steel and to 1.3 μm in the 0.4% C steel. The phase transformation during high temperature tempering is accompanied by recovery and subgrain coalescence. Depending on the carbon content, a tensile strength of 1700–1900 MPa or 650–750 MPa can be achieved after tempering at 450°C or 800°C, respectively.

Keywords: Martensitic stainless steels, quenching, tempering, retained austenite, strength.

INTRODUCTION

Metallic materials used for medical instruments are required certain physical properties like corrosion resistance, magnetic properties, etc [1]. Concurrently, materials in medicine should have assured mechanical properties [2, 3]. Although ordinary mechanical strength is enough for structural steels and alloys for the most of applications in medicine, some medical instruments experience significant loads and, therefore, must have high yield and tensile strengths. The dental instruments are one of such sustainable application, which should withstand high stresses. The high strength can be obtained in tempered steels. However, plain carbon steels have a significant disadvantage in the form of low corrosion resistance. This disadvantage can be overcome by using stainless steels [4] commonly represented by nickel-chromium steels with an austenitic structure, which provides high corrosion resistance. In the case of high strength requirement, martensitic steels with high chromium content are used [5, 6]. A typical high-strength stainless steel is AISI 420, which has been developed for industries that require high hardness/strength values and the ability to work in mildly aggressive environments. Another important feature of materials subjected to processing on automatic machines is their machinability, which is usually improved by increasing the sulfur content. Increasing the sulfur content has little effect on corrosion resistance. In addition, steels are additionally alloyed with niobium and molybdenum to eliminate the possible negative effect of sulfur on impact toughness. Regarding the usage of automatic machining, the steel semi-products must have hardness below about 250 HV, which is achieved through appropriate heat treatment. Then the high strength of the final products should be obtained by subsequent ending treatment. Therefore, advanced steels for dental instruments should possess a wide range of strength properties that could be controlled by a rather simple heat treatment.

According to our previous study [7], suitable strength levels in 420-type steels can be obtained by tempering at 450°C for 3 h (hardness above 520 HV) or at 800°C for 16 h (hardness below 250 HV). However, the effect of alloying extent on the developed microstructures was not clarified. Therefore, the aim of the present study is to analyze the effect

¹Belgorod National Research University, Belgorod, Russia, e-mail: dolzhenko_p@bsu.edu.ru, mishnev@bsu.edu.ru, belyakov@bsu.edu.ru; ²Russian State Agrarian University – Moscow Timiryazev Agricultural Academy, Moscow, Russia, e-mail: kajbyshev@rgau-msha.ru. Original article submitted October 27, 2023.

TABLE 1. Alloying Content of the Studied Steels (wt.%)

Steel	C	Si	Mn	P	S	Cr	Mo	Nb
20Cr13	0.24	1.13	1.17	<0.0001	0.2	12.43	0.56	0.08
30Cr13	0.33	1.1	1.2	<0.0001	0.15	13.4	0.58	0.06
40Cr13	0.4	1.2	1.0	<0.0001	0.18	14.0	0.6	0.04

of heat treatment on the microstructures and the mechanical properties of modified AISI 420-type steels designated for automatic machining. In particular, the study is focused on the tempered microstructures and their influence on the strength of the steels with different carbon content ranging from 0.2 to 0.4%.

MATERIAL AND METHODS

Three steels with different nominal carbon content of 0.2, 0.3, and 0.4% designated as 20Cr13, 30Cr13, and 40Cr13, respectively, were studied. The chemical compositions of the studied steels are presented in Table 1. The steels were annealed at 1050°C for 10 min in nitrogen environment followed by air quenching. Then, the steel samples were tempered at 450°C for 3 h or at 800°C for 16 h using a conventional muffle furnace.

The structural investigations were carried out using a Quanta 600 scanning electron microscope (SEM) equipped with automatic analyzer of electron backscattering diffraction patterns incorporating an orientation imaging microscopy (OIM) system. The SEM specimens were prepared by electro-polishing at a voltage of 25 V using 1:9 solution of perchloric acid in acetic acid. The grain size was measured by a linear intercept method as a high-angle grain/phase boundary spacing using orthogonal grid with TSL OIM Analysis 6 software. In addition to OIM, the volume fraction of retained austenite was evaluated by X-ray diffraction and magnetic induction methods using a Rigaku SmartLab diffractometer and a Feritscope FMP30, respectively [8]. Then the volume fraction of retained austenite was averaged over OIM, X-Ray, and magnetic methods. The tensile tests were carried out using an Instron 5882 universal testing machine and specimens with a cross section of $3 \times 1.5 \text{ mm}^2$ and a gauge length of 12 mm.

RESULTS AND DISCUSSION

The microstructures and properties of the present steels depend substantially on the fraction of retained austenite. The volume fraction of retained austenite after quenching increased from 0.14 to 0.38 when the carbon content increased from 0.2 to 0.4%. Tempering was accompanied by the phase transformation. A series of X-Ray diffraction patterns observed for the steel samples after tempering at 450°C for 3 h is shown in Fig. 1.

The fraction of retained austenite in the samples tempered at 450°C decreases and comprises 0.09 in 20Cr13 steel, 0.34 in 30Cr13 steel, and 0.28 in 40Cr13 steel. An increase in the tempering temperature to 800°C promotes the phase transformation. The retained austenite completely disappears after tempering at 800°C for 16 h.

Typical tempered microstructures evolved in the studied steel samples are shown in Figs. 2–4 along with the phase and grain/phase boundary misorientation distributions. The 20Cr13 steel sample tempered at 450°C for 3 h is characterized by typical martensitic-like microstructure with a relatively small amount of retained austenite uniformly distributed throughout the sample (Fig. 2). An average grain size is 0.97 μm .

The corresponding grain/phase boundary misorientation distribution includes three peaks for small misorientations below 5° and around 45° and 60°. The small misorientations correspond to numerous low-angle subboundaries of the lath martensite origin. The sharp peak around 60° results from specific misorientations between the martensite packets and the blocks that frequently appears in steels upon martensitic transformation [9, 10]. The peak around 45° should be related to the interphase boundaries between tempered martensite and retained austenite [11].

In contrast, almost equiaxed microstructure with a grain size of 2.1 μm develops in this steel after tempering at 800°C for 16 h. Tempering at such a high temperature as 800°C is accompanied by the recovery of the dislocation substructure, including polygonization and subgrain coalescence in the tempered martensite as well as partial

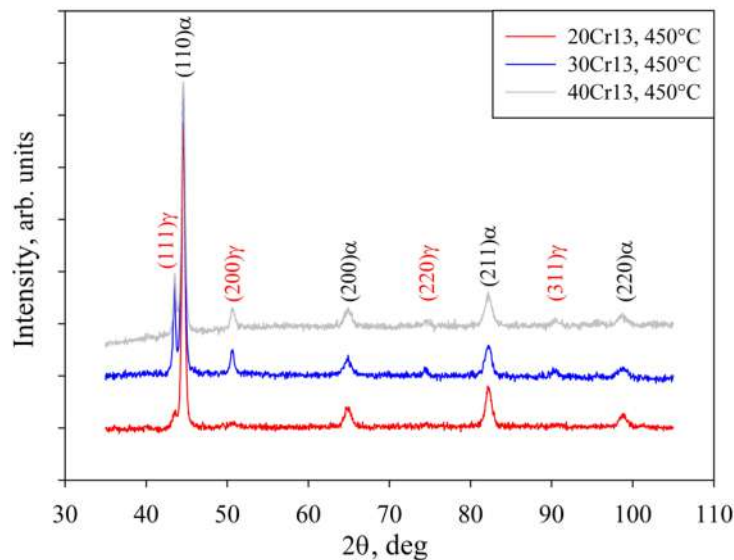


Fig. 1. X-Ray diffraction of the martensitic stainless steels tempered at 450°C for 3 h.

recrystallization/grain growth. As a result of the austenite-ferrite transformation and the recrystallization/grain growth, the peaks corresponding to small misorientations and those around 45° decrease remarkably in the misorientation distribution. The latter, therefore, involves only peaks for large misorientations around 50° and 60° related to the misorientations between transformation variants [9, 10].

The 30Cr13 steel samples contain much larger fraction of retained austenite (0.34) after tempering at 450°C for 3 h (Fig. 3). The tempered martensite in the 30Cr13 steel samples is characterized by a finer microstructure compared to that in the 20Cr13 samples. The average grain size in the 30Cr13 steel samples is about 0.71 μm or 1.7 μm after tempering at 450°C or 800°C, respectively. The misorientation distributions of the grain/subgrain/phase boundaries in the 30Cr13 steel sample after tempering at 450°C consist of three sharp peaks for small misorientations resulted from the martensite lath boundaries, 45° misorientations associated with the interphase boundaries of retained austenite/martensite, and 60° misorientations of the transformation variants. It is worth noting that the peak of 45° misorientations significantly exceeds other peaks due to the large fraction of retained austenite in the 30Cr13 steel sample after tempering at 450°C. On the other hand, the grain/subgrain boundary misorientation distribution in the 30Cr13 steel sample after tempering at 800°C for 16 h looks similar to that in the 20Cr13 steel. Namely, the misorientation distribution is characterized by relatively large fractions of 50° and 60° misorientations. Such misorientation distribution can be attributed to the phase transformation accompanied with ferrite recovery and recrystallization.

The tempered microstructures in the 40Cr13 steel samples are qualitatively the same with those in the 20Cr13/30Cr13 steels (Fig. 4). Quantitatively, the microstructures developed in the 40Cr13 steel samples are differentiated by finer grains with a size of 0.6 μm after tempering at 450°C or 1.3 μm after tempering at 800°C. It should be noted that the tempered microstructures in the 40Cr13 steel sample subjected to 800°C treatment consists of much more equiaxed grains compared to those in 20Cr13/30Cr13 steels. The development of the equiaxed ultrafine grained microstructure during high temperature tempering may result from the dispersed martensite/retained austenite microstructure in the 40Cr13 steel after quenching. Almost the same fractions of retained austenite in the 30Cr13 and 40Cr13 steels are responsible for the similar misorientation distributions among the microstructures evolved by tempering at 450°C. In contrast to the microstructures tempered at 450°C, those tempered at 800°C are less affected by the fraction of retained austenite. Almost the same grain/subgrain boundary misorientation distributions are observed after tempering at 800°C for 16 h in the steel samples irrespective of the carbon content.

A series of the tensile stress vs elongation curves for the specimens made of tempered steels is shown in Fig. 5.

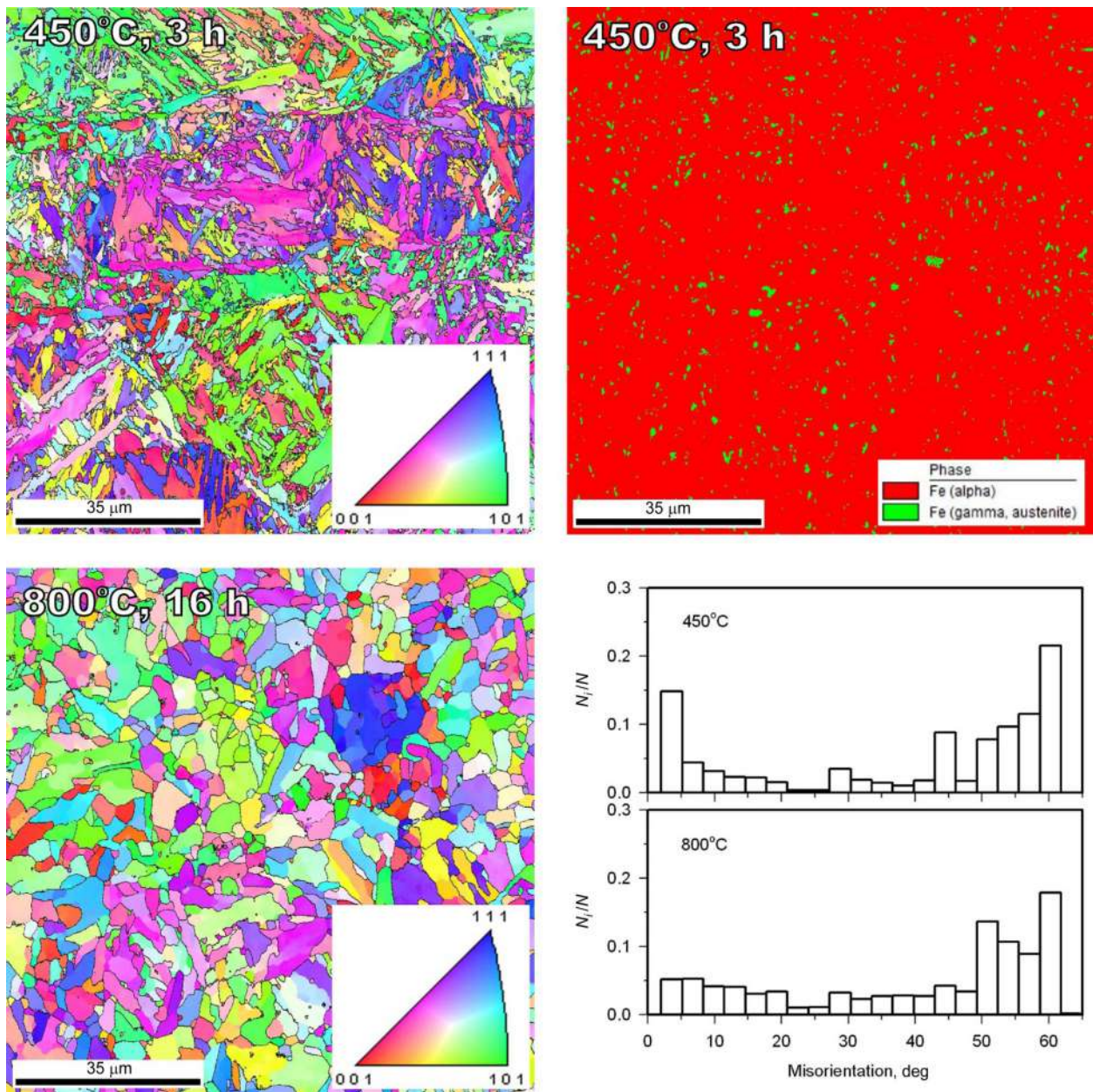


Fig. 2. Tempered microstructures, austenite/martensite phase map, and boundary misorientation distribution for 20Cr13 stainless steel tempered under the indicated conditions.

The curves can be categorized in two domains. The steels tempered at 450°C for 3 h exhibit high strength in the range of 1700–1900 MPa depending on the carbon content. On the other hand, the tempering at 800°C for 16 h results in ultimate tensile strength (UTS) of 650–750 MPa. An increase in the carbon content in the studied steels commonly increases the strength including both yield strength and UTS. Note here that the effect of the carbon content on the strength is more pronounced after tempering at 450°C. It is interesting that the fraction of retained austenite does not affect significantly the mechanical properties of steels after tempering at 450°C. The high strength well above 1500 MPa after 450°C tempering seems to be mainly attributed to the carbon effect, which is responsible to the combined strengthening by solid solutions, dislocations, and dispersed particles. Note here that among the different strengthening mechanisms, the dislocation strengthening was considered as the main contributor to the total strength

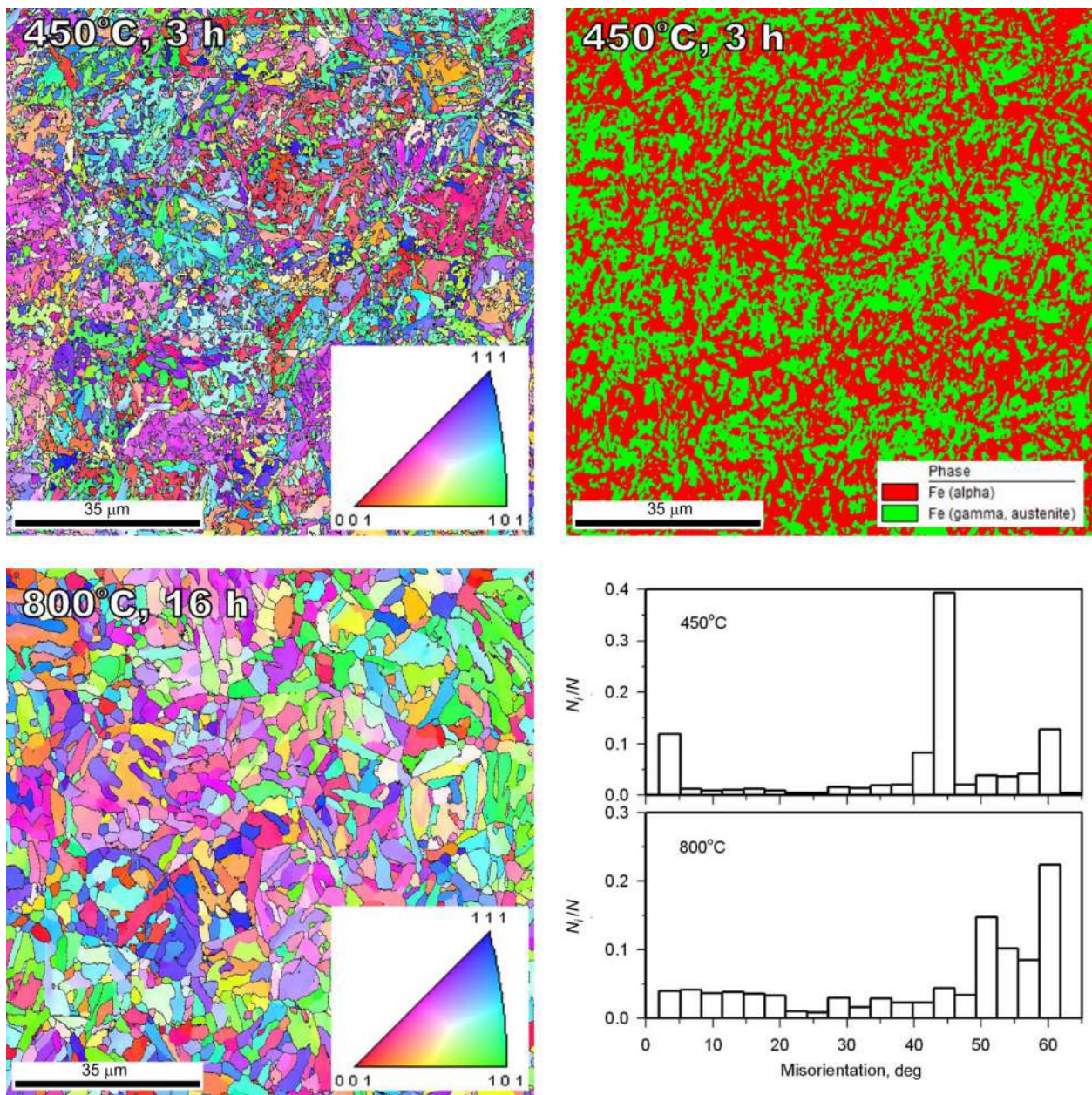


Fig. 3. Tempered microstructures, austenite/martensite phase map, and boundary misorientation distribution for the 30Cr13 stainless steel tempered under the indicated conditions.

[7]. On the other hand, a relatively low tensile strength below 750 MPa after 800°C tempering can be related to the ferrite recovery and recrystallization following the complete decomposition of austenite/martensite, when the indirect effect of the carbon content on the grain size and carbide dispersion results in minor changes in the strength.

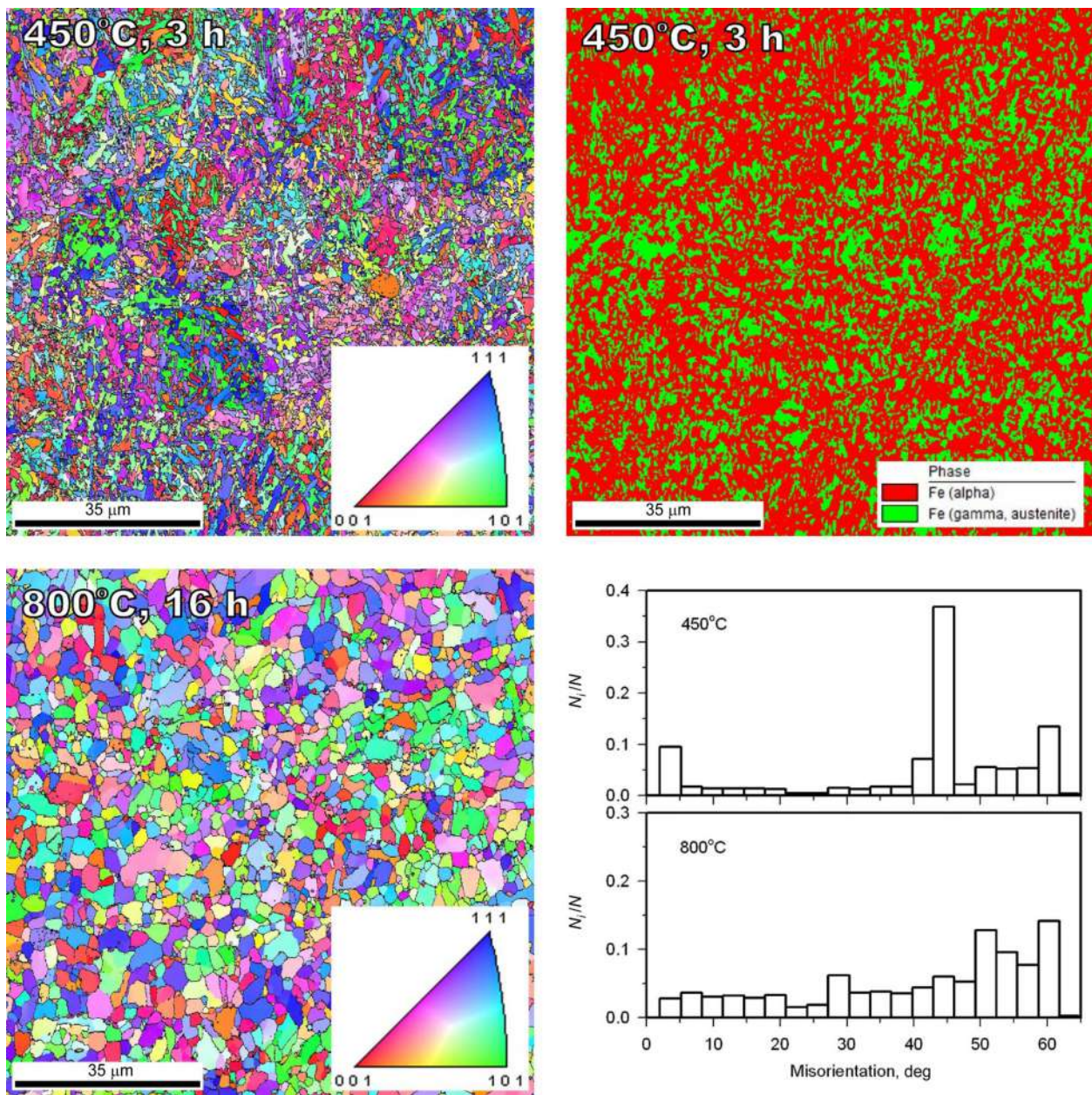


Fig. 4. Tempered microstructures, austenite/martensite phase map, and boundary misorientation distribution for 40Cr13 stainless steel tempered under the indicated conditions.

CONCLUSIONS

The effect of tempering conditions on the microstructure and the strength of the AISI 420-type martensitic stainless steels with carbon content in the range from 0.2 to 0.4% has been studied. The main results can be summarized as follows.

1. The volume fraction of retained austenite depends significantly on the carbon content. The fraction of retained austenite after air quenching increased from 0.14 to 0.38 as the carbon content increased from 0.2 to 0.4%.

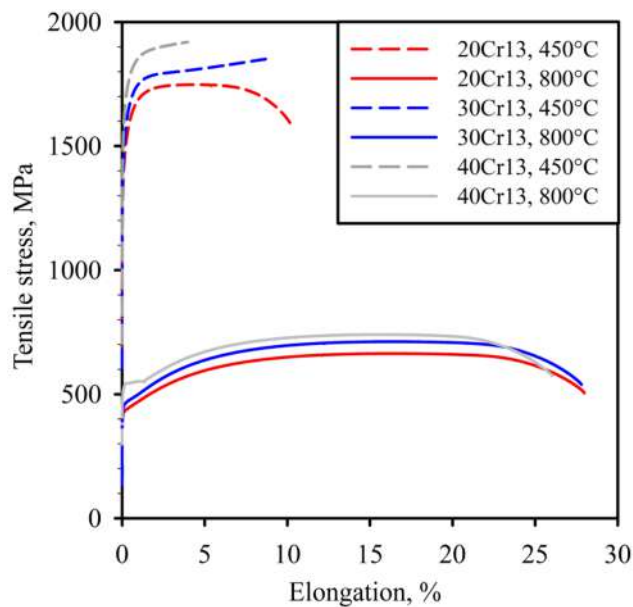


Fig. 5. Tensile stress-elongation curves for the martensitic stainless steels tempered at the indicated temperatures.

Tempering at 450°C for 3 h reduced the fraction of retained austenite to 0.09 and 0.28 in the steels with 0.2 and 0.4% of carbon, respectively. Retained austenite completely removed after tempering at 800°C for 16 h.

2. The average grain size comprised 0.97 μm and 0.6 μm after tempering at 450°C for 3 h in the steels with carbon content of 0.2 and 0.4%, respectively. The corresponding grain/subgrain/phase boundary misorientation distributions were characterized by large fractions of low-angle subboundaries and high-angle boundaries with misorientations around 45° and 60°. Tempering at 800°C for 16 h increased the grain size to 2.1 μm in the 0.2% C steel and to 1.3 μm in the 0.4% C steel. The phase transformation during high temperature tempering was accompanied by recovery and subgrain coalescence. Thus, the evolved misorientation distribution included large fractions of high-angle boundaries with misorientations of around 50° and 60° inherent in the phase transformation.

3. Depending on carbon content, the tensile strength of 1700–1900 MPa was achieved after tempering at 450°C for 3 h in the studied steels. On the other hand, the tensile strength in the range of 650–750 MPa was obtained after high temperature tempering at 800°C for 16 h.

COMPLIANCE WITH ETHICAL STANDARDS

Author contributions

R.O.K., R.V.M., P.D.D., and A.N.B. conceived of the presented idea; P.D.D. and R.V.M. developed the theory and performed the computations; P.D.D. and A.N.B. verified the analytical methods; and R.O.K. encouraged A.N.B. to investigate and supervised the findings of this work. All authors discussed the results and contributed to the final manuscript. All authors have read and agreed to the published version of the manuscript.

Conflicts of interest

The authors declare that they have no known competing financial interests or personal relationships that could have appeared to influence the work reported in this paper.

Funding

The research was funded by the Ministry of Science and Higher Education of the Russian Federation under the Agreement No. 07511-2021-046 (IGK 000000S407521QLP0002) with SEZ JSC “VladMiVa” under the complex Project “Organization of a High-Tech Production of Export-Oriented Medical Devices Based on Innovative Structural Materials for the Purpose of Import Substitution Based on Developed Technologies.”

Financial interests

The authors have no relevant financial or non-financial interests to disclose.

Institutional review board statement

Applicable.

Acknowledgments

The authors thank the National Research University BelSU for help in implementation of research, development, and technological works using the equipment of the Center for Collective Use “Technologies and Materials of NRU BelSU.”

REFERENCES

1. S. V. Kulkarni, A. Nemade, and P. D. Sonawwanay, In: Recent Advances in Manufacturing Processes and Systems. Lecture Notes in Mechanical Engineering, H. K. Dave, U. S. Dixit, and D. Nedelcu, eds., Springer, Singapore (2022); DOI: 10.1007/978-981-16-7787-8_11.
2. Z. Horak, K. Dvorak, L. Zarybnicka, *et al.*, *Materials*, **13**, 4560 (2020); DOI: 10.3390/ma13204560.
3. V. Kh. Sabitov, *Medical Instruments, Medicine*, Moscow (1985).
4. K. H. Lo, C. H. Shek, and J. K. L. Lai, *Mater. Sci. Eng. R Rep.*, **65**, 39 (2009); DOI:10.1016/j.mser.2009.03.001.
5. W. Martienssen and H. Warlimont, eds., *Springer Handbook of Condensed Matter and Materials Data*, Springer, Heidelberg; New York (2005).
6. K. Saeidi, D. L. Zapata, F. Lofaj, *et al.*, *Addit. Manuf.*, **29**, 100803 (2019); DOI: 10.1016/j.addma.2019.100803.
7. V. Torganchuk, P. Dolzhenko, L. Polovneva, and R. Kaibyshev, *AIP Conf. Proc.*, **2899**, 020145 (2023); <https://doi.org/10.1063/5.0164166>.
8. R. Mishnev, Yu. Borisova, S. Gaidar, *et al.*, *Metals*, **13**, 689 (2023); DOI: 10.3390/met13040689.
9. H. Kitahara, R. Ueji, M. Ueda, *et al.*, *Mat. Char.*, **54**, 378 (2005); DOI: 10.1016/j.matchar.2004.12.015.
10. H. Kitahara, R. Ueji, N. Tsuji, and Y. Minamino, *Acta Mater.*, **54**, 1279 (2006); DOI: 10.1016/j.actamat.2005.11.001.
11. Y. He, S. Godet, and J. J. Jonas, *J. Appl. Cryst.*, **39**, 72 (2006); DOI: 10.1107/S0021889805038276.